16th World Conference on Earthquake, 16WCEE 2017
Santiago Chile, January 9th to 13th 2017
Paper N° 3236 (Abstract ID)
Registration Code: S-V1460835018

EVALUATION OF REINFORCED CONCRETE WALL–FLAT SLAB CONNECTION WITH A NOVAL DUCTILE DETAILING

S.R. Salim[(1)], K.P. Jaya[(2)]

[(1)] *Assistant Professor, Department of Civil Engineering, SRM University, surumirazia@gmail.com*
[(2)] *Professor, Structural Engineering Division, Anna University, jayakp@annauniv.edu*

Abstract

This paper presents the investigations carried out to study the performance of shear wall-flat slab joint region with a novel detailing pattern. An experimental investigation of behaviour of two identical wall-flat slab joint subassemblies was conducted by testing joint models with overall dimensions of 2.4m (height) × 0.84m (width): one with conventional reinforcement detailing at the joint and the other with a proposed novel reinforcement detailing at the joint region under lateral seismic type loading. Moreover, three-dimensional nonlinear finite element models of the wall-flat slab joint subassembly with the two types of reinforcement detailing at the joint region were developed and analyzed using ABAQUS/CAE software. It was observed that the proposed novel reinforcement detailing for structural wall-flat slab joint region for the construction of shear wall structures exhibited improved ductility in the joint region ensuring increased energy dissipation which is desired under seismic loading.

Keywords: shear wall – flat slab connection; reinforcement detailing; seismic loading; joint shear; ductility

1. Introduction

1.1 Statement of the problem

Earthquake resistant design of structures has gained much importance as earthquake is off late not so rare. In order to build earthquake resistant structures, considerable research and dissemination of information is necessary in the design and detailing of structural elements as well as connections. The connection between shear wall and floor slab is an essential link in the lateral load resisting mechanism of wall - slab systems. The performance of the connection can influence the pattern and distribution of lateral forces among the vertical elements of the structure. There exists need for study about simple and proper detailing of connections under seismic loading. By modifying the joint detailing pattern, seismic performance of the connection can be improved to a great extent. Research works have been reported with proposed reinforcement detailing options at the wall–slab joint region under lateral loading. Siti and Yee [1] reported the effect of layered reinforcement in the wall on bending capacity for support stiffness in wall slab system. Later, Al-aghbari et al. [2] studied and compared the structural performance of cross and anchorage bracings under out-of-plane lateral cyclic loading. Greeshma & Jaya [3,4] reported works with proposed type of detailing with cross bars, hook bars, and shear reinforcements in slabs; in which the effectiveness of cross bars at the joint was proved under torsional loading.

Even though the significance of the wall - slab connections in sustaining large deformations and forces during earthquakes is enormous, specific detailing guidelines are not explicitly available as codal provisions. The existing recommendation as per ACI 318 M-02 [5] and BS EN 1998-1 [6] regarding the detailing of wall to slab joint is the provision of additional standard U hooks connecting the shear wall and slab for a lap length equal to the development length of the bar. However, the joint performance can be enhanced by altering the 'void joint core' due to the U hooks. For this purpose, a noval ductile detailing with additional shear reinforcement (connecting the consecutive U hooks) in the joint core region has been proposed. The present paper analyses some test results, relevant to two subassemblies' units tested under static reverse cyclic loads, to evaluate the effect of the proposed joint detailing on the behaviour of shear wall to floor slab joint region. Successively, three-dimensional nonlinear finite element models of the wall- slab joint subassembly were developed and analyzed using ABAQUS/CAE software.

1.2 Load transfer in wall-slab systems

In the wall-slab systems, the shear walls and floor slabs act together as a rigid jointed frame in resisting loads. Generally, in shear wall structures, the two orientations of primary elements in the load path are: vertical (shear wall, braced frame and moment frame) and horizontal (roof, floors and foundation).

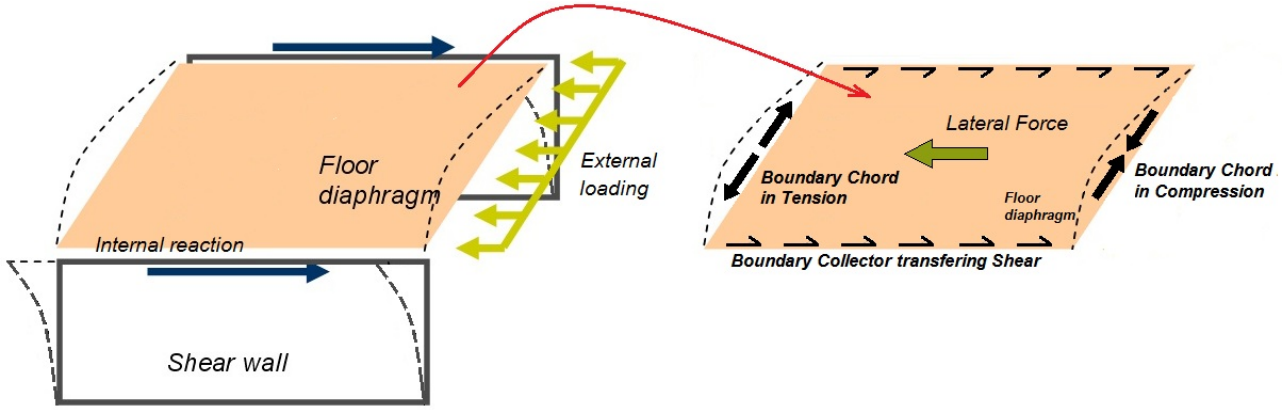

Fig. 1 – Primary structural load path

Within the primary load-path elements, there are individual secondary elements needed to provide specific pathways along which lateral forces are transmitted. Two important secondary elements are chords and collectors. A chord is a structural member along the boundary of a diaphragm that resists tension and compression forces. A collector is a structural member that transmits diaphragm forces into shear walls or frames. The overall functioning of chords and collectors is shown in Fig.1. The forces acting perpendicular to the boundary elements tend to bend the diaphragm and the chord member resists the associated tension and compression. Walls that structurally support diaphragm edges also resist out-of-plane forces caused by diaphragm bending.

The deformed shape of the shear wall structure under lateral loading is shown in Fig.2. Due to the lateral loading, the exterior shear wall-slab subassembly is subjected to in plane moment at the slab-wall joint. This in-plane moment can be simulated through a couple acting at the end of the slab.

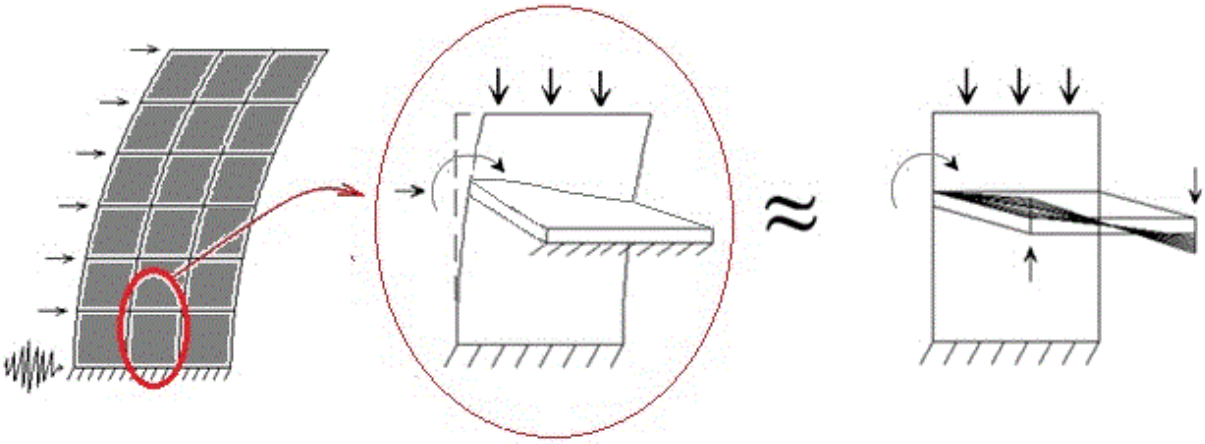

Fig. 2 – Simulation of joint forces

2. Test Units

2.1 Geometry and reinforcement

The typical first storey exterior wall - slab subassembly was taken as the test unit for the study. The test unit included ground storey shear wall, a portion of first floor slab (based on yield line analysis) and the first storey shear wall. The test units were of one-third scaled down models of the designed exterior wall - slab subassembly. Two test units: one with conventional reinforcement detailing at the joint and the other with a proposed novel reinforcement detailing at the joint region were developed.

Both the test units were of same dimensions with a 835x83.5 mm slab connected to a shear wall of 2417x835x100 mm. The slab projection was 500 mm from the face of shear wall. In order to apply the axial load, an additional projection of 500 mm was provided at the top of the shear wall. The clear concrete cover thickness was 10 mm and 15 mm for the slab and shear wall respectively. The dimensions and reinforcement details of the test units are shown in Fig.3 (a) and (b).

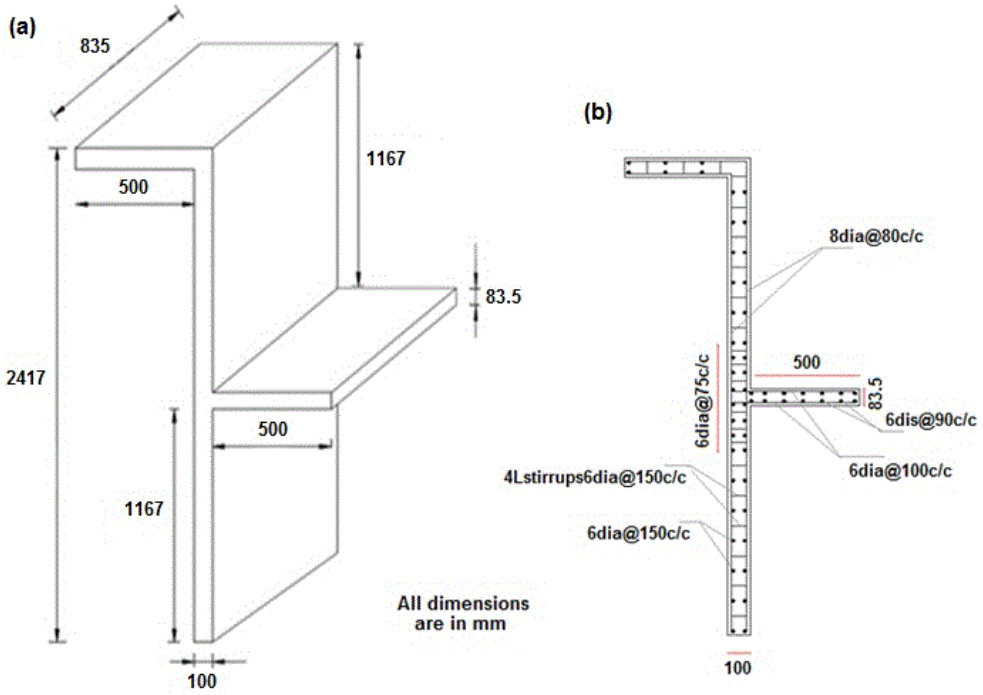

Fig.3 – (a) Geometry of test units; (b) Reinforcement details of the test units.

The two units had the same reinforcement detailing for the shear wall and slab. The subassembly labeled "U" was constructed with conventional reinforcement detailing at the wall slab joint region, i.e. the provision of U shaped hooks connecting the shear wall and the slab for a lap length equal to development length of the bar (Ld), from the inner side of the wall. While the other subassembly labeled "A" has been constructed with proposed non-conventional reinforcement detailing, viz. additional core shear reinforcement at the joint region. In order to modify the void joint core of conventional reinforcement detailing, stirrups are provided in the joint core connecting the U hooks. The joint reinforcement details of the test units are shown in Fig.4.

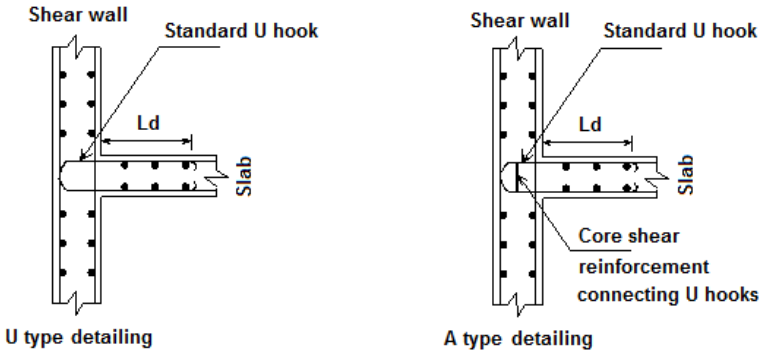

Fig.4 – Connection detailing of the test units

2.2 Development of test units

The reinforcing steel bar bending was carried out to obtain the desired detailing of the shear wall - floor slab joint. The views of reinforcement cages are shown in Figure 5. For reinforcement of the test units, Fe 415 grade steel was used. The yield strength of 6 mm and 8mm steel bars was 489.3 N/mm^2 and 458.5 N/mm^2 respectively. The concrete mix was designed according to IS 10262:1982 [7] in proportion of 1:1.27:2.39 by weight of cement, fine aggregate and coarse aggregates respectively. Portland cement of 53 grade was used for casting the

test units. River sand passing through 4.75 mm IS sieve and having a fineness modulus of 2.73 was used as fine aggregate. Crushed granite stone of maximum size not exceeding 10 mm and having a fineness modulus of 6.09 was used as coarse aggregate. A slump of 100 mm was used to accommodate any steel congestion in the joint region. The average compressive strength of concrete cubes after 28 days of curing was 37.76 N/mm^2.

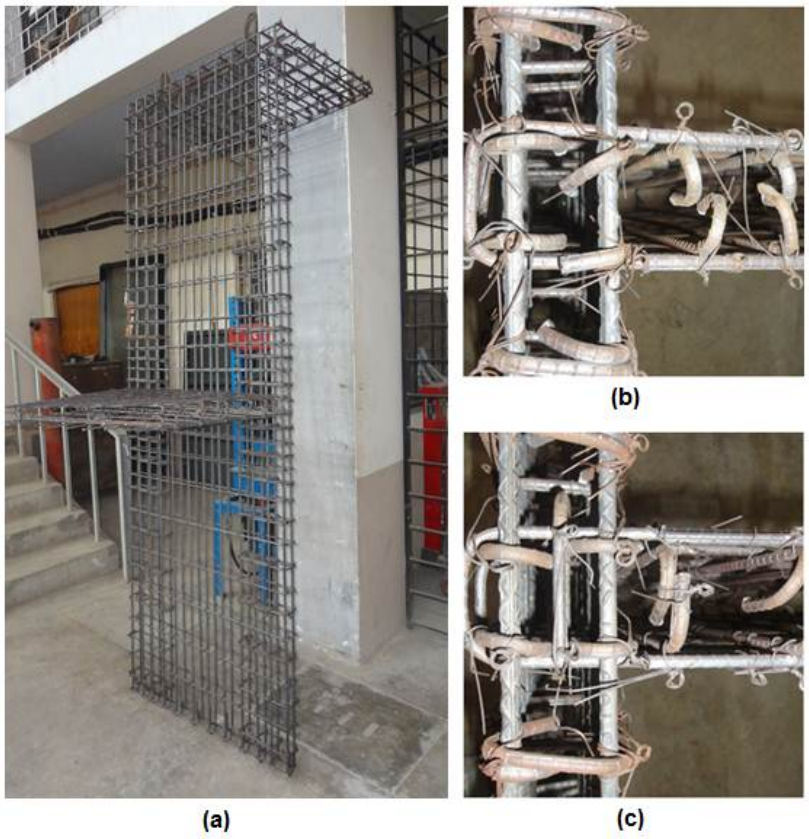

Fig.5 – (a) View of reinforcement cage; (b) Joint detailing of test unit U; (c) Joint detailing of test unit A.

2.3 Test setup and loading history

The test units were tested in a well- equipped setup as shown schematically in Fig. 6. The shear wall was fixed at the bottom by attaching it to two steel channels using four high-strength threaded rods. The steel channels were properly anchored to the strong test floor. The top of the shear wall was restrained for displacements in both directions to ensure complete shear transfer at the joint. A total load of 8 kN was applied by assembling cubes to simulate the axial load at the second storey height. The units were tested under displacement controlled system subjected to reverse cyclic loading up to failure. The pattern of cyclic displacements applied by the hydraulic jack during test is given in Fig. 6. To apply the simulated reverse cyclic load on the units, 100-kN capacity hand-controlled hydraulic jacks (four numbers) were connected to a reaction steel frame. Four hydraulic jacks were linked to the top and bottom of the slab ends as shown in Fig. 6. The units were subjected to an increasing displacement in a cyclic manner up to failure. The displacement amplitude at the end of the slab was increased by steps of 0.5 mm up to a displacement of 2 mm, then by steps of 1 mm up to failure, with 3 cycles for each amplitude levels. The loading sequence was observed using load cells with least count of 10 kg for applying cyclic load. The units were instrumented with load cells, dial gauges, and strain gauges to monitor the behaviour of units during testing. Fig. 7 shows the view of test in progress.

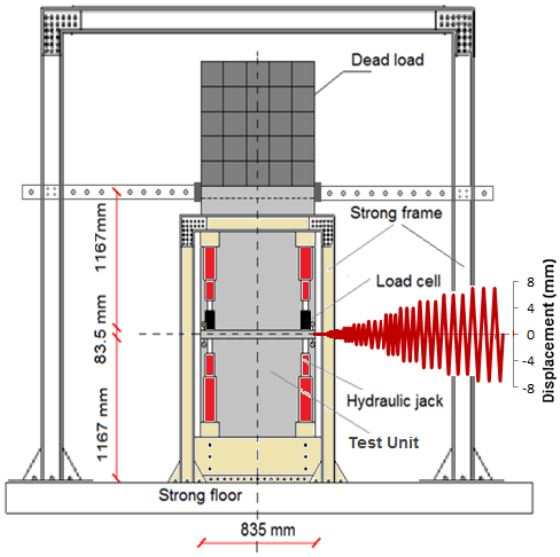

Fig.6 – Test setup and loading

Fig.7 – View of test in progress

3. Test Results

In this section, the test results are presented in terms of strength and load–displacement hysteresis with a discussion of the relevant failure mechanisms. The variation in ultimate load and moment carrying capacities of the wall - slab subassemblies with the two types of detailing subjected to both positive and negative direction of reverse cyclic loading is shown in Table.1. The test unit A exhibited 31.5% and 28.1% greater load carrying capacity than the conventional test unit U in the positive and negative direction respectively.

Table 1 - Comparison of ultimate load and moment carrying capacity of test units

Designation of test unit	Ultimate Load (kN)		Ultimate moment (kNm)	
	Positive direction	Negative direction	Positive direction	Negative direction
U	37.8	34.5	18.9	17.25
A	49.7	44.2	24.85	22.1

The hysteretic behaviour of both the test units is depicted in Fig. 8. The presence of the core shear reinforcement increased the slab resistance capacity in tension and compression as confirmed from the hysteresis loops, thereby demanding additional wall strength in both directions of loading. The areas of the hysteresis loops gradually became larger as the displacement cycle increased, which indicated good energy dissipating capacity. An increase of 112% was observed in cumulative energy dissipation capacity for test unit with A type detailing when compared with the conventional test unit U. The ductility generally measured in terms of displacement ductility is calculated as per the ASCE guidelines [8] from the load-displacement envelope curve. The average displacement ductility factor calculated for the test units U and A were 1.61 and 2.40 respectively. Thus the displacement ductility was enhanced by 49% for the test unit with proposed non-conventional detailing than that of the conventional one.

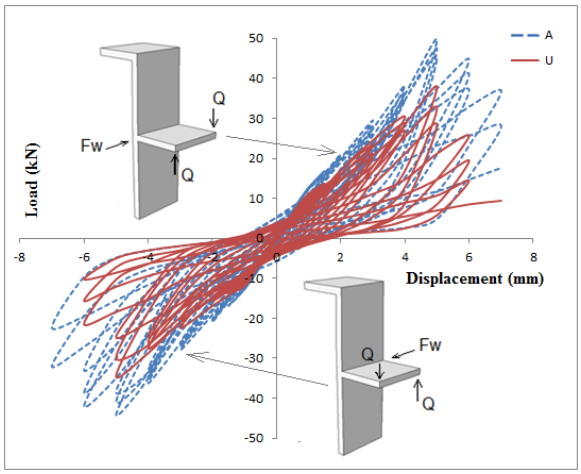

Fig.8 – Experimental hysteretic behaviour of the test units

The two test units at failure are displayed in Fig.9, where the different crack patterns can be observed. For the test unit U, initial cracks were developed in the slab diagonally from the loading points, which progressively developed towards the joint. The initial diagonal hairline crack occurred at the joint when the displacement reached 5 mm. Thereafter, the existing diagonal cracks widened and more cracks kept on developing in the slab and joint. In the non-linear region of the response, subsequent cracking occurred for higher loading cycles at the joint interface, slab region and in the shear wall also. The test unit failed due to the widening of crack at the interface between slab and shear wall.

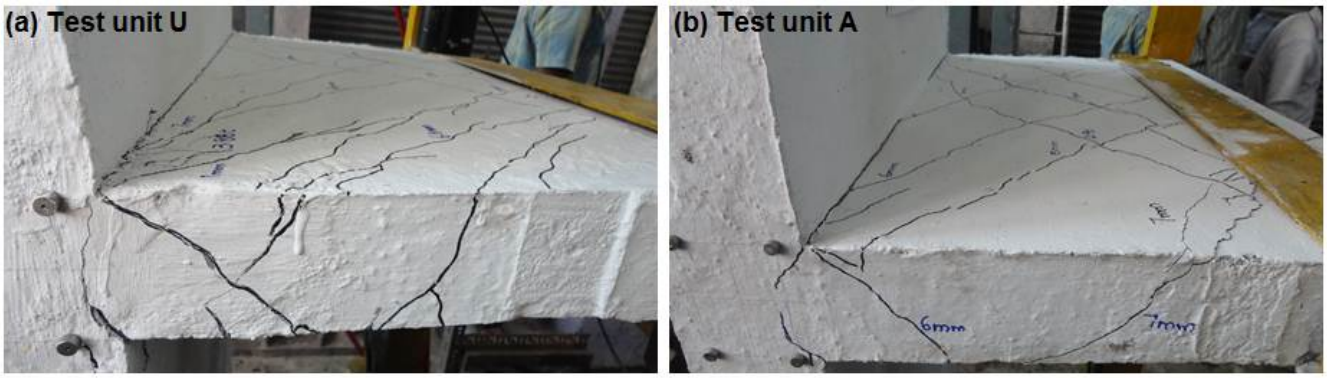

Fig.9 – Crack pattern of test units.

In the case of test unit A, no major cracks were noticed at the joint, and the joint remained intact throughout the loading cycle. The core shear reinforcement at the joint region were capable of resisting tensile stresses developed in the joint region due to cyclic loading, and hence, only few hairline cracks were noticed at the joint region. No visible cracks were observed in the shear wall. The developed cracks in the slab kept on widening on higher drift cycles followed by the progressive redistribution of forces leading to final failure of the slab. The test unit A failed due to the widening of cracks at the slab. A comparison of crack pattern in both the test units showed that the additional shear reinforcement stirrups in the joint core region are capable of resisting tensile stresses at the joint.

4. Numerical Simulation

4.1. Numerical model and relevant material properties

The behaviour of the test units was simulated numerically by means of the nonlinear 3D finite element models depicted in Fig.10. The models were designated as U and A, with conventional and proposed type of detailing

respectively. The models were built using the well-known general purpose finite element program ABAQUS [9]. The concrete was modelled with 3D 8-node solid elements (C3D8R, hexagonal eight-node brick) and every reinforcing bar was modelled using beam elements (B31, two-node linear beam). The mechanical properties of the reinforcing steel were described by means of ABAQUS's standard elasto-plastic model using nonlinear isotropic/kinematic hardening. The mechanical properties of concrete were modelled using ABAQUS's own Concrete Damage Plasticity (CDP) formulation. The compression and tension response input data for M30 concrete enables the calculation of the hardening and stiffening variables by ABAQUS. The compression hardening data and the tension stiffening data were provided in terms of crushing strain and cracking strain respectively for M30 grade concrete.

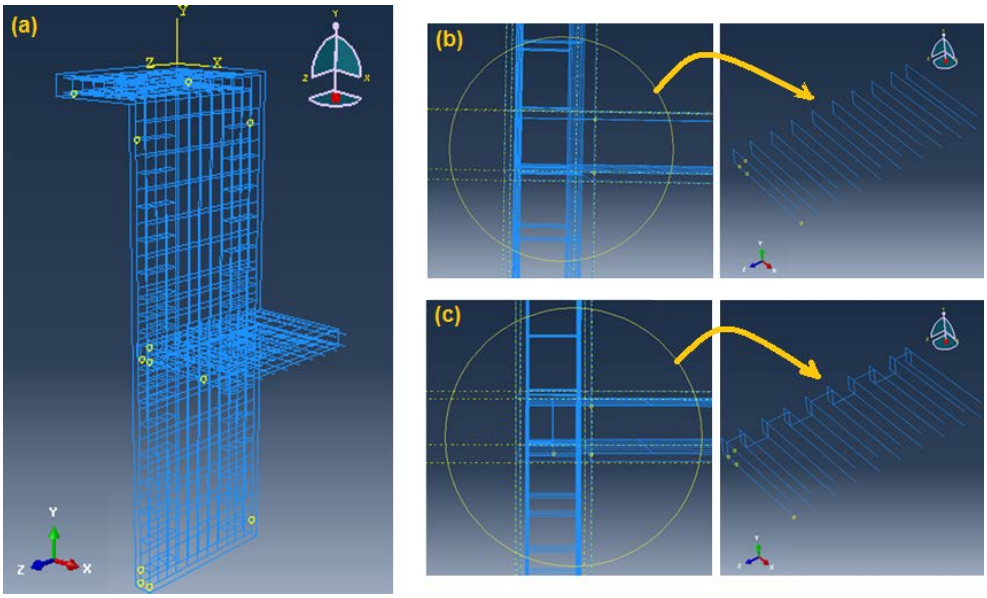

Fig.10 – (a) FE model of wall-slab subassembly; (b) Model of U type joint; (c) Model of A type joint.

The interaction between the steel bars was ensured by merging all the steel bars, which produced a tie constraint at every point of contact between two steel bars. Full bond between concrete and reinforcement was assumed using the embedded region constraint interaction between steel and concrete sections. This interaction constrains the translational degree of freedom of the nodes of the embedded elements with respect to the response of the host elements.

4.2. Finite element analysis

The shear wall was assumed to be fixed at the base. For this, all degrees of freedom were constrained at the base of the shear wall. The top of the shear wall was restrained for in plane and out of plane movement. The axial load at the top of the subassembly was distributed as pressure at the top face of the model. The boundary conditions and loading of the subassembly are shown in Fig. 11. The displacement controlled loading was achieved by defining partitions of circular profile (of same dimensions of the load cell as in the case of test conducted) and assigning the prescribed displacement to the partitions. The partitions were assigned to the same displacement cycles as in the loading history of the test conducted. The prescribed displacement was achieved by using amplitude function (smooth step) in the boundary condition module. The analysis was performed in two steps. In the first step the response due to gravity loading has been evaluated and subsequently, in the second step, the response due to cyclic loading has been evaluated. A complete run of the software using one of the fastest available Personal Computers took 48 hours.

4.3. Model validation

To facilitate the comparison of the experimental and numerical study, load-displacement envelope was obtained by plotting between the maximum load sustained in each cycle and corresponding displacement. Fig. 12 shows the comparison of the load-displacement envelope curves of both the joint models. A satisfactory agreement

between the numerical and experimental results is observed. The numerical results were found to be higher than the experimental results and the variation in the results was within 11%. The models could predict the capacity and behaviour of the joint sub-assemblage quite well. The provision of reinforcement in the core region has been proven to be effective from the measured and computed similar values under cyclic loading. The measured and computed displacement ductility also shows the improvement for model with reinforcement in the joint core, confirming that the model works well.

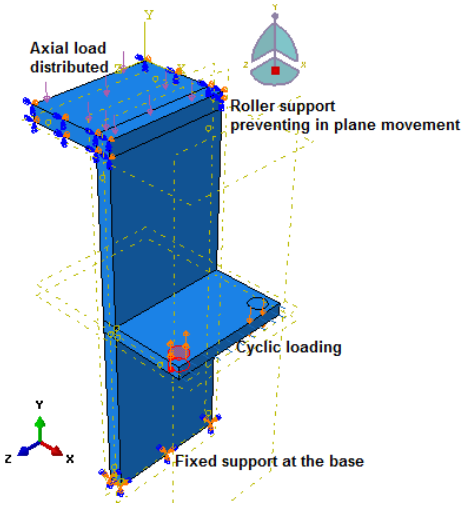

Fig.11 – Loading and boundary conditions of the model.

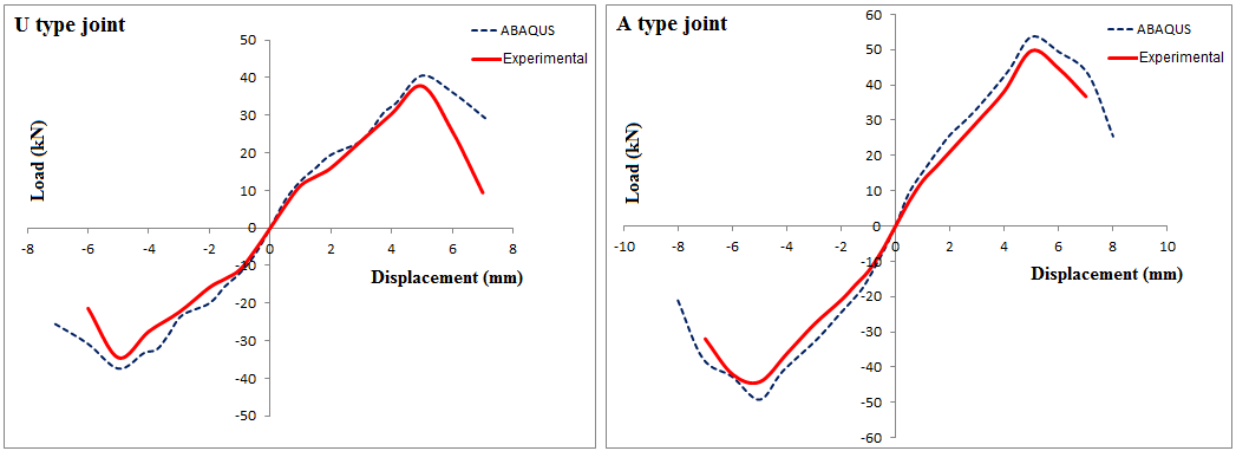

Fig.12 – Comparison of load-displacement envelope.

5. Numerical Results

In this section, the numerical results are presented in terms of strength, load–displacement hysteresis and joint stress with a discussion of the obtained contours plots. The variation in ultimate load and moment carrying capacities for the two categories of detailing for both positive and negative direction of loading is shown in Table 2. The model A exhibited 32.3% and 31.5% greater load carrying capacity than the conventional U model in the positive and negative direction respectively. The load-displacement hysteresis loops for the cyclic loading at each displacement excursion level of the two models are shown in Fig. 13. The models exhibited fat hysteresis loops with very less pinching, due to good bonding between reinforcement and joint concrete. The displacement ductility factor was calculated for both the models from the load-displacement envelope curve. The average displacement ductility factor of the models U and A were 1.75 and 2.49 respectively. Thus, the displacement ductility was found to be enhanced by 42% for model A when compared with model U.

Table 2 - Comparison of ultimate load and moment carrying capacity of numerical models.

Designation of model	Ultimate Load (kN)		Ultimate moment (kNm)	
	Positive direction	Negative direction	Positive direction	Negative direction
U	40.6	37.4	20.3	18.7
A	53.7	49.2	26.85	24.6

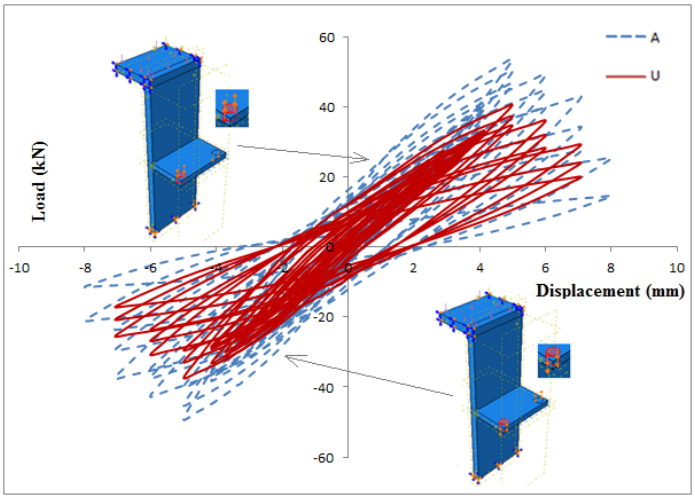

Fig.13 – Hysteretic behaviour of the numerical models.

A comparison of the von mises stress in the joint bars is shown in Fig. 14. An increased stress level was observed in the model A due to the effect of stirrups in the core, and is resisted within the joint. It was observed that the hooks of the conventional model U at the joint region have got stressed to some extent thereby developing damage at the interface between slab and shear wall. In the model A, the stirrups confined the joint core ensuring uniform distribution of stresses into the vertical element bars.

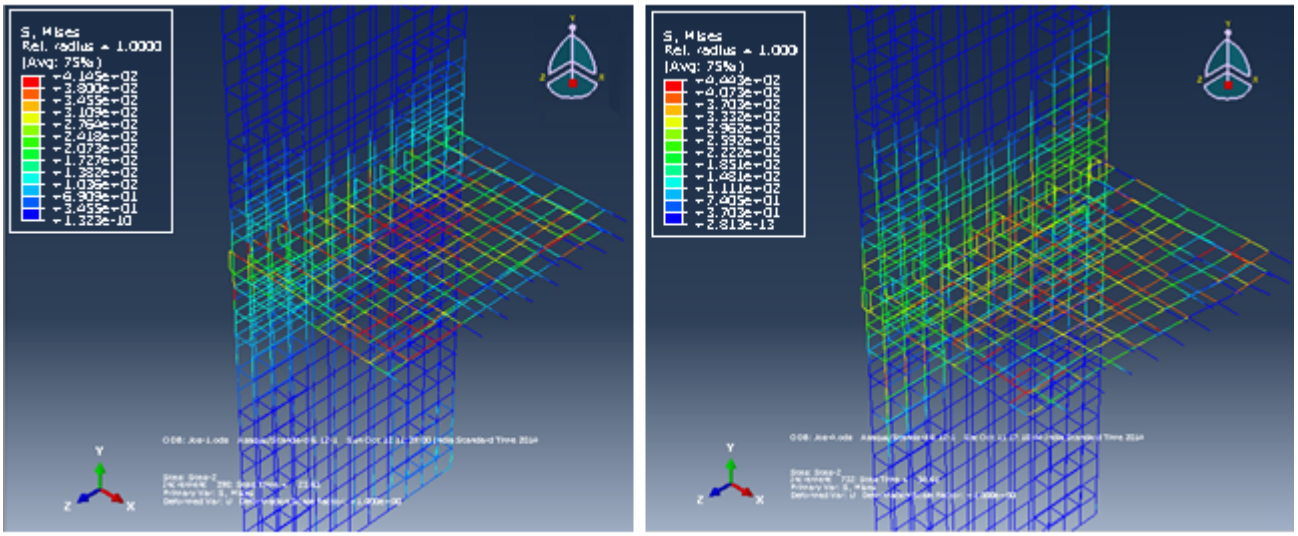

Fig.14 – Joint stress of the numerical models.

The maximum inelastic deformation of the model A under reverse cyclic loading is presented in Fig. 15. The deformed shape of the model was observed to be similar to that in the experimental study. The contour diagrams of shear stress for the positive loading direction at 8mm displacement cycle of model A are presented in Fig. 16. It was observed that the model could reflect the expected response of the joint subassembly in terms of deformations and stresses.

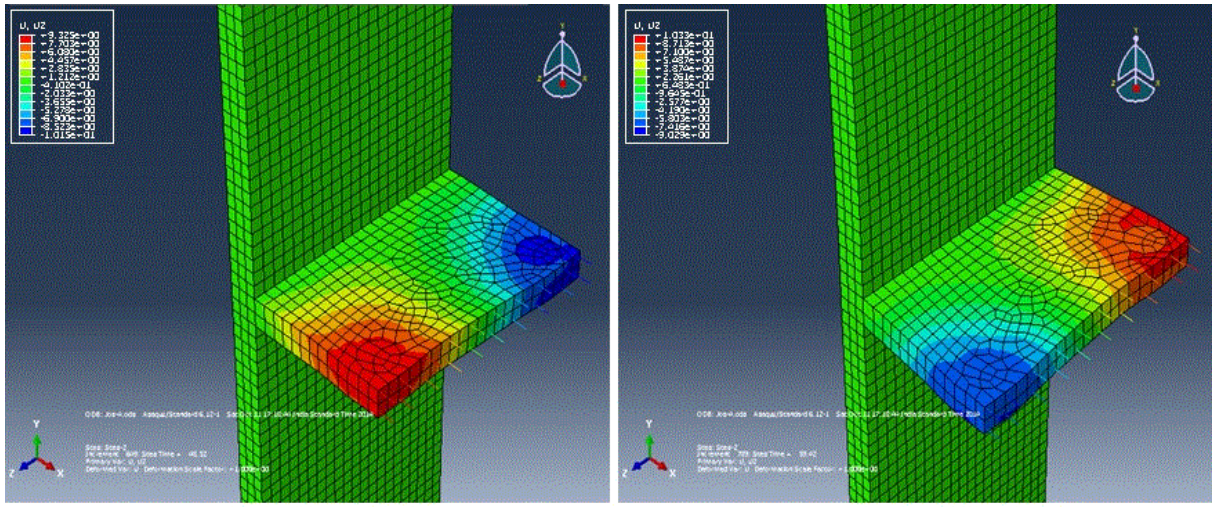

Fig.15 – Maximum deformation of numerical model A.

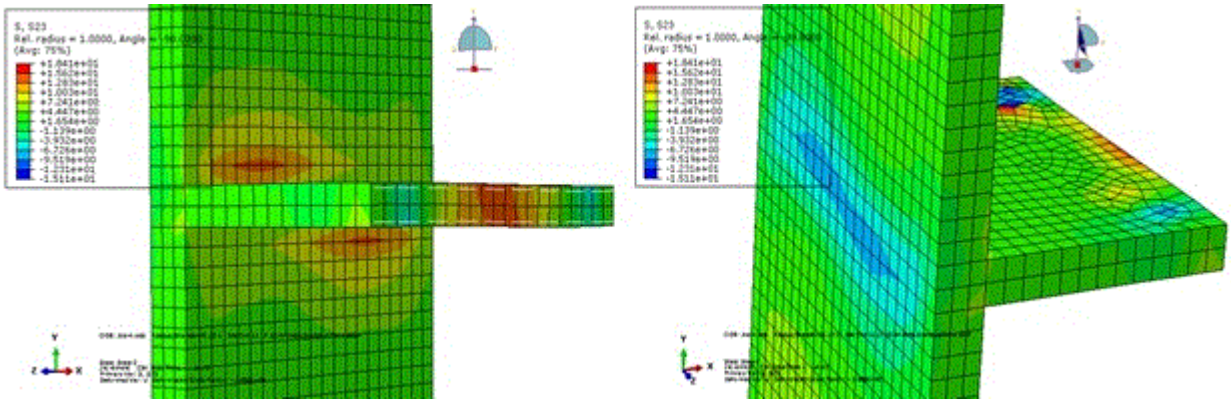

Fig.16 – Shear stress contour numerical model A

6. Conclusions and Outlook

Wall- slab joint subassembly with the proposed core shear reinforcement was able to undergo large inelastic deformations while ensuring an easier constructability and superior post-earthquake functionality compared to the conventional counterpart. The shear reinforcement in the core region could take care of the joint shear demands by arresting the tensile forces due to shear. The shear reinforcement also would provide increased confinement of the joint core region. The effect of such confinement of concrete core, increased shear taking capacity and better anchorage provides increased overall capacity of the joint region. The tests and the numerical simulations demonstrated the following:

1. The joint subassembly with A type detailing (shear reinforcement in the core region) exhibited a maximum of 31.5% and 32.3 % higher load carrying capacity than that of the conventional U type joint in the experimental and numerical studies respectively. The numerical results were in close comparison with the experimental findings with a reasonable level of overestimation, where the variation in the results was within 11%.

2. The enhancements in deformation capacity for A type joint was 49% and 42% from experimental and numerical investigations respectively when compared with that of U type joint. The enhancement in cumulative energy dissipation from experimental investigation for A type joint was observed to be 112% higher than that of the conventional joint.
3. The joint remained intact throughout the loading cycle for the subassembly with A type detailing. The core shear reinforcement at the joint region was capable of resisting tensile stresses developed in the joint region due to cyclic loading and hence, only few hairline cracks were noticed at the joint region. No visible cracks were observed in the shear wall. This proves that subassembly with A type detailing satisfies the fundamental requirement of strong wall-weak slab concept.

Thus, the present study has proven the effectiveness of the provision of core shear reinforcement as a viable ductile detailing for the construction of the wall - slab joint in seismic risk regions.

7. References

[1] Siti, I., Yee, H., M.: An Investigation on effect of Rebar on Structural behaviour for wall-slab system, IEEE Business, Engineering & Industrial applications Colloquium (BEIAC), (2012), No.978-1-4673-0426-9/12, pp. 26-29.

[2] Al-aghbari, A., Hamid, N., Rahman, N and Hamzah, S.: Structural Performance of two types of wall slab connection under out-of-plane lateral cyclic loading, Journal of Engineering science and technology, 7 (2012) 2, pp. 177-194.

[3] Greeshma, S., Jaya, K., P.: Effect of Cross inclined bars on the behaviour of shear wall-floor slab joint under lateral cyclic loading, Journal of Structural Engineering (2012) Special Issue, April, Ref. No. 320(28/B)/2012/JOSE.

[4] Greeshma, S., Jaya, K., P., Rajesh, C.: Seismic Behaviour of Shear Wall – Slab Joint under Lateral Cyclic Loading, Asian Journal of Civil Engineering (Building andhousing), 13 (2012) 4, pp. 455-464.

[5] ACI Committee 318 - 2002, 'Building Code Requirements for Structural Concrete (ACI 318-02)', American Concrete Institute, Detroit.

[6] BS EN 1998-1(2004), 'Eurocode 8: Design of Structures for Earthquake Resistance - Part 1:General Rules, seismic actions and rules for buildings'.

[7] IS 10262-1982: Recommended Guidelines for Concrete Mix Design, Bureau of Indian Standards, New Delhi, India.

[8] ASCE 31-03: 2002, 'Seismic evaluation of existing buildings', New York, USA.

[9] Abaqus 6.12: Abaqus/CAE user's manual version, Dassault Systèmes, Dassault Systèmes Simulia Corp., Providence, RI, USA, 2012.